Published in final edited form as:
Clin Cancer Res. 2010 March 15; 16(6): 1834–1844. doi:10.1158/1078-0432.CCR-09-3123.

Targeted inhibition of inducible nitric oxide synthase inhibits growth of human melanoma *in vivo* and synergizes with chemotherapy

Andrew G. Sikora[a,b,e,1], **Alexander Gelbard**[a,b,d,1], **Michael A. Davies**[a,f], **Daisuke Sano**[b], **Suhendan Ekmekcioglu**[c], **John Kwon**[c], **Yared Hailemichael**[*], **Padmini Jayaraman**[e], **Jeffrey N. Myers**[b], **Elizabeth A. Grimm**[c], and **Willem W. Overwijk**[a,2]

[a] UT MD Anderson Cancer Center: Dept. of Melanoma Medical Oncology, 1515 Holcombe Blvd, Unit 430, Houston, TX 77030

[b] UT MD Anderson Cancer Center: Dept. of Head and Neck Surgery, 1515 Holcombe Blvd, Unit 430, Houston, TX 77030

[c] UT MD Anderson Cancer Center: Dept. of Experimental Therapeutics, 1515 Holcombe Blvd, Unit 430, Houston, TX 77030

[d] Bobby Alford Department of Otolaryngology, Baylor College of Medicine, One Baylor Plaza, Houston, TX 77030

[e] Departments of Otolaryngology, Immunobiology, Oncological Sciences, and Dermatology, Mount Sinai School of Medicine, One Gustave L. Levy. Place, Box 1189, New York, NY 10029

[f] UT MD Anderson Cancer Center: Dept. Of Systems Biology, 1515 Holcombe Blvd, Unit 430, Houston, TX 77030

Abstract

Purpose—Aberrant expression of inflammatory molecules, such as inducible nitric oxide synthase (iNOS), has been linked to cancer, suggesting that their inhibition is a rational therapeutic approach. While iNOS expression in melanoma and other cancers is associated with poor clinical prognosis, *in vitro* and *in vivo* studies suggest that iNOS and nitric oxide (NO) can have both pro-and anti-tumor effects. We tested the hypothesis that targeted iNOS inhibition would interfere with human melanoma growth and survival *in vivo* in a preclinical model.

Experimental design—We used an immunodeficient NOD/SCID xenograft model to test the susceptibility of two different human melanoma lines to the orally-administered iNOS-selective small molecule antagonist N6-(1-Iminoethyl)-L-lysine-dihydrochloride (L-nil)with and without cytotoxic cisplatin chemotherapy.

Results—L-nil significantly inhibited melanoma growth and extended the survival of tumor-bearing mice. L-nil treatment decreased the density of CD31+ microvessels and increased the number of apoptotic cells in tumor xenografts. Proteomic analysis of melanoma xenografts with

2CORRESPONDING AUTHOR: WWO (woverwijk@mdanderson.org; Phone: 713-563-5294; Fax: 713-563-3424).. AGS (andrew.sikora@mssm.edu; Phone: 212-659-9516; Fax: 212-369-5701).

[1]The first two authors contributed equally to the work described in this manuscript.

STATEMENT OF TRANSLATIONAL RELEVANCE:

Currently there is no reliably effective “standard of care” treatment for advanced melanoma. In this study, we demonstrate that the small molecule iNOS inhibitor L-nil has potent anti-melanoma activity, and can be effectively used in combination with cytotoxic chemotherapy in vivo. Since L-nil and related drugs have previously been used in non-cancer human studies, targeted iNOS inhibition has great potential for translation to clinical trials for melanoma and other solid tumors.

reverse-phase protein array (RPPA) identified alterations in the expression of multiple cell signaling and survival genes after L-nil treatment. The canonical anti-apoptotic protein Bcl-2 was downregulated *in vivo* and *in vitro* after L-nil treatment, which was associated with increased susceptibility to cisplatin-mediated tumor death. Consistent with this observation, combination therapy with L-nil plus cisplatin *in vivo* was more effective than either drug alone, without increased toxicity.

Conclusions—These data support the hypothesis that iNOS and iNOS-derived NO support tumor growth *in vivo*, and provide convincing preclinical validation of targeted iNOS inhibition as therapy for solid tumors.

INTRODUCTION

Upregulation of pro-inflammatory molecules by tumor cells is a poorly understood phenomenon which can play a role in both the induction and maintenance of certain human cancers(1). One such molecule, inducible nitric oxide synthase (iNOS) is constitutively over-expressed in many cancers, including melanoma and gastric(2), breast(3), colon(4), and head and neck(5,6)carcinomas. iNOS and its product NO have wide-ranging and varied effects on cellular physiology, signal transduction, and cell survival. At high levels, such as produced by activated macrophages during inflammatory responses to pathogens, NO alone or in combination with reactive oxygen species (ROS) can have a direct cytotoxic effect on pathogens or tumor cells(7). At lower levels, NO can affect signal transduction pathways by interacting with metal ligands of proteins (8)or covalently modifying proteins through nitration and nitrosylation (9,10). These protein modifications can increase or decrease enzyme activity, or enhance protein stability depending on the specific amino acid residues modified, the amount of available NO, the redox status of the cell, and the availability of protein substrates(9,10). As NO can modulate numerous signal transduction pathways in cancer cells via post-translational protein modification, iNOS expression can potentially serve as a global regulator of carcinogenesis and tumor behavior.

A link between iNOS and cancer development and progression has been proposed, based on both clinical and experimental evidence. On balance, data from *in vivo* tumor models and cell culture studies support a link between iNOS/NO and carcinogenesis, tumor progression, tumor survival, and aggressiveness (reviewed in (11–13)) but results vary greatly depending on the experimental model used. *In vitro*, low-level NO production, such as is produced by many human tumor cells, seems to support tumor growth and survival by a variety of mechanisms including enhancing the stability of the anti-apoptotic protein Bcl-2 via s-nitrosylation (14), and inhibiting the pro-apoptotic activity of caspase-3(15). In both *in vitro* and *in vivo* models, iNOS and NO have been variously shown to enhance carcinogenesis and tumor progression, stimulate angiogenesis, support tumor growth, promote metastasis, and inhibit T cell-dependent immune responses (reviewed in (16,13,11). Thus there is substantial interest in iNOS and NO as therapeutic targets for cancer therapy.

Malignant melanoma is among the fastest-growing causes of cancer death, responsible for roughly 68,720 new cases and 8,650 deaths in the US in 2009(17). While early-stage disease is generally treatable by surgery, there is no consistently effective treatment for metastatic disease. In melanoma, iNOS expression is absent in benign nevi and present in invasive melanoma (18), and the level of expression correlates strongly with poor clinical outcome (19,20). *In vitro* data supports the ability of NO to protect human melanoma cells from apoptosis, and NO depletion enhances sensitivity to cisplatin (21). Thus, both clinical and *in vitro* evidence supports the hypothesis that targeted inhibition of iNOS and iNOS-derived NO may be an effective therapeutic approach for melanoma and other iNOS-expressing tumors.

In the present study, we tested the effect of iNOS inhibition with small-molecule antagonists on human melanoma *in vivo* using a xenograft model. We found that the iNOS selective antagonist N6-(1-iminoethyl)-L-lysine dihydrochloride(L-nil)(22)inhibited iNOS-dependent NO production by human melanoma cells in a dose-dependent fashion *in vitro*, and strongly suppressed melanoma growth *in vivo* without evident toxicity. Growth suppression was associated with a decrease in tumor microvessels, downregulation of the anti-apoptotic gene Bcl-2, increased number of intratumoral apoptotic cells, and enhanced efficacy when L-nil treatment was combined with cisplatin *in vivo*. These data suggest that iNOS-selective small molecule inhibitors, alone or in combination with conventional cytotoxic chemotherapy, are a promising approach to therapy of melanoma and other solid tumors.

MATERIALS AND METHODS

Western Blots

Cell lysates were separated by size using SDS-PAGE and transferred to a membrane. Membranes were incubated with a primary antibody against iNOS (sc-651, Santa Cruz Biotech), Bcl-2 (Pharmingen), or ERK2 (sc-154, Santa Cruz) followed by a secondary antibody conjugated to horse radish peroxidase (HRP). Relative signal intensities for Bcl-2 were validated by Western blot, and normalized densitometry values expressed as ratio of Bcl-2 to ERK2 protein levels.

Tumor Cell lines and Transient Transfection

The human melanoma cell lines mel624 and mel528 were a kind gift from Dr. J. Wunderlich, Surgery Branch, National Cancer Institute, NIH, Bethesda, MD. The A375 human melanoma line was purchased from ATCC. The human colon line WiDR was a kind gift of J Hodge, Laboratory of Tumor Immunology and Biology, National Cancer Institute, NIH, Bethesda, MD. WIDR cells were transfected with lipofectamine according the manufacturer's (Invitrogen) protocol.24 hours after transfection cells were re-plated for use in the indicated assays. Plasmid expressing the gene encoding full-length human iNOS protein was a generous gift from Keping Xie, and has been previously described(23). All melanomalines were submitted to the Characterized Cell Line Core, of the MD Anderson Cancer Center Support Grant (http://inside.mdanderson.org/departments/ccsg/characterized-cell-line-core/charcell.html). Fingerprinting analysis is performed and cells are validated every two years; the lines in this study were validated in March 2008.

Detection of Nitric Oxide and in vitro Inhibitor Experiments

Cell lines were cultured in phenol free Dulbecco's modified Eagle medium supplemented with 10% fetal bovine serum, penicillin & streptomycin at 37°C in 5% CO_2. 2×10^5 cells were cultured in a 24 well plate with the indicated concentration of L-NIL for 72 hours before assay for cell death or NO levels. Cumulative NO production was measured *in vitro* by the nitrite reconversion method with the Apollo 4000 bioanalyzer (World Precision Instruments, Sarasota, FL)as previously described(24). In cytotoxicity experiments the XTT cell proliferation assay (Cayman Chemical, Ann Arbor, MI) or Annexin/PI cell death assay (BD Biosciences, San Jose, CA) was used according to the manufacturer's directions.

For *in vivo* NO measurements, C57BL/6 mice received 0.1% L-nil in drinking water or plain water control for 48 hours prior to intraperitoneal injection of 250 μg LPS. Mice were sacrificed at 7 hours post-injection, and serum prepared from whole blood by centrifugation. Serum was then clarified by passage through a 10 KD cutoff spin-filter (Millipore, Billerica, MA) and nitrite levels determined by Griess assay(25).

L-nil was obtained from A.G. Scientific (San Diego, CA). Griess reagent, 1,3-PBIT, lipopolysaccharide and aminoguanidine were obtained from Sigma Aldrich Corp. (St. Louis, MO).

Intracellular Bcl-2 staining

Staining with anti-Bcl-2 antibody was modified from the published protocol(26). In brief, cells were permeabilized using cytofix/cytoperm kit (BD PharMingen)and stained with Bcl-2-FITC antibody or matched isotype control (BD PharMingen).

Animals In vivo Tumor Experiments

Female NOD/SCID mice(ages 6–8 weeks) were purchased from the Animal Production Area of the National Cancer Institute-Frederick Cancer Research and Development Center. Female C57BL/6mice(ages 6–8 weeks) were purchased from JAX labs. The mice were bred and maintained in a pathogen-free environment and fed irradiated mouse chow and autoclaved reverse osmosis-treated water. All of the animal procedures were done in accordance with a protocol approved by the Institutional Animal Care and Use Committee of the University of Texas MD Anderson Cancer Center. In xenograft experiments, animals were injected with human melanoma tumor cell lines (either mel624 or A375), at initial concentrations of 5×10^6 cells or 7.5×10^6 cells in 100 μL PBS respectively. Animals were randomized after tumors established, and assigned to experimental groups (10/group unless otherwise noted). Experimental animals received 0.15% or 0.2% L-NIL or 0.2%PBIT in their drinking water, replaced every 2–3 days, beginning 3 days after tumor implantation. Control animals received plain drinking water. In some experiments, animals received cisplatin administered at the indicated dose and time point via intraperitoneal injection. Animals were weighed regularly and monitored for signs of toxicity. Tumor growth was measured three times per week using electronic calipers, and tumor volumes determined by multiplying the longest axis by its perpendicular. Mice were humanely sacrificed when tumors reached >250 mm^2, ulceration occurred, or mice become moribund. In some tumor experiments, representative animals were evaluated by magnetic resonance imaging (MRI) using a 7.0 T Biospec USR small animal imaging system (Bruker Biospin MRI, Billerica, MA). A linear volume resonator with 35 mm inner diameter (ID) was used for signal excitation and detection. Axial T1-weighted (TE/TR 8.5ms/900ms, 2 averages, 156nm × 156nm × 1mm resolution) and T2-weighted images (TE/TR 65ms/5000ms, RARE factor 12, 3 averages) with matching slice prescriptions were collected for tumor visualization.

Immunohistochemistry

Paraffin-embedded sections of excised human melanoma tumor xenografts were examined for Nitrotyrosine (NT) and iNOS expression by immunohistochemistry using an anti-NT polyclonal antibody (Upstate Biotechnology, Lake Placid, NY) or anti-iNOS monoclonal antibody (BD-Transduction Laboratories). Pre-immune normal rabbit IgG (Vector Laboratories, Burlingame, CA) and anti-vimentin antibody (BioGenex Laboratories, San Ramon, CA) were used as negative and positive controls, respectively. Tissue sections were deparaffinized and rehydrated, then placed in Antigen Unmasking Solution (Vector Laboratories) and microwaved intermittently for a total of 10 min, to maintain boiling temperature. After cooling, the slides were placed in 3% H_2O_2 in cold methanol for 15 min, and then 0.05% Triton X-100 (Sigma, St. Louis, MO) for 15 min. An avidin-biotin-peroxidase complex (ABC) kit (Vectastain, Vector Laboratories) was then used for antigen detection according to the manufacturer's instructions and the immunolabeling developed with the chromogen 3-amino-9-ethylcarbazole for 10 min.

For detection of CD31, frozen tumor sections were fixed in cold acetone for 10 min prior to immunostaining withanti-CD31 primary antibody(PharMingen)for 1 h at room temperature,

detection with peroxidase-conjugated secondary antibody, and counterstaining with hematoxylin. Terminal deoxynucleotidyl transferase-mediated dUTP nick end labeling (TUNEL)assay was performed on paraformaldehyde-fixed tissues with an apoptosis detection kit (Promega, Madison, WI)according to the manufacturer's direction. CD31/TUNEL double-staining was performed by subjecting the same tissues to sequential CD31 immunostaining with Alexa Fluor 594-conjugated secondary antibody, and TUNEL assay with fluorescein-dUTP.

Quantification of NT, iNOS, Microvessel Density, Apoptotic Tumor, Mean Vessel Diameter, and Endothelial Cells

Immunofluorescence microscopy images were obtained with a Leica DMLA microscope (Leica Microsystems, Bannockburn, IL)to equipped with a Hamamatsu 5810 cooled CCD camera (Hamamatsu Corp., Bridgewater, NJ) and ImagePro Plus 6.0 software (Media Cybernetics, Silver Spring, MD). Photomontages were prepared using Adobe Photoshop software (Adobe Systems, Inc., San Jose, CA). For the quantification analysis, four slides were prepared for each group. The percentage of positively-staining cells in each group were calculated and compared. For quantification of TUNEL expression, the cells positively stained were counted in 5 random 0.04-mm^2 fields at 200X magnification per slide. To quantify microvessel density (MVD), areas containing higher numbers of tumor-associated blood vessels were identified at low microscopic power (100X). Vessels completely stained with anti-CD31 antibodies were counted in 5 random 0.159-mm^2 fields at 100X magnification per slide. For comparison of vessel diameter between control and experimental groups mean diameter in pixels was calculated for the stained blood vessels in 10 random 0.159-mm2 fields at 100X magnification.

Reverse Phase Protein Array

RPPA as performed has been described previously(27)and was used to quantify protein and phospho-protein expression of 59 cancer-related and signal transduction proteins including Bcl-2, phospho-PDK1 ($^{(}Ser^{241)}$, phosphor-AMPK ($Thr^{172)}$, 4EBP1, P7056K, S6, TSC2, PTEN, mammalian target of rapamycin (mTOR), and others. Comparison Anitbodies were from Cell Signaling, Beverly, MA(PTEN, mTOR and all phospho-specific antibodies), Epitomics Inc., Burlingame, CA (total p70S6K antibody); and DAKO, Carpinteria, CA(Bcl-2).

Statistical analysis

The quantifications of the immunohistochemical expression of NT, iNOS, TUNEL, microvessel density, and mean vessel diameter were compared by the paired Student's *t*-test, with significance at $P < 0.01$. For *in vitro* experiments, student's T test and a significance threshold of $P<0.05$ was used. For *in vivo* survival experiments, Kaplan-Meir survival curves were generated and significant differences determined using the log-rank test. In vivo tumor growth curves were compared using the nonparametric method of Koziol, et al to allow comparisons despite unequal survival of mice between groups (28).

RESULTS

Human melanoma lines express iNOS and release NO, which is inhibited by the selective antagonist L-nil

Western blot analysis was used to screen melanoma cell lines for iNOS protein expression (Fig 1A), using the previously confirmed iNOS-negative colon cancer cell line WIDR(4)as a negative control. iNOS protein was strongly expressed in the melanoma lines mel526 and A375, and expressed less strongly in mel624. iNOS expression was maintained *in vivo*, as

A375 tumor xenografts were strongly positive for both iNOS and the stable NO end product nitrotyrosine by immunohistochemistry (Fig 1B). The presence of nitrotyrosine demonstrates that iNOS is expressed and catalyzes NO production in human melanoma cells.

As basal NO production by melanoma lines was consistently at the lower limit of detection of the relatively insensitive Griess assay, further NO measurements were made with the TBI 4100 electrochemical nitric oxide probe (WPI instruments), which is capable of measuring nanomolar levels of NO. All iNOS-positive melanoma lines produced nanomolar levels of NO (Fig 2A). Basal NO levels in media from WIDR cells (which do not express iNOS mRNA)(29)were just above those of medium alone; after transfection with an iNOS-encoding expression plasmid, WIDR/iNOS cells released NO at levels comparable to melanoma cells. The iNOS-selective competitive antagonist L-nil, when added to culture medium, inhibited NO release by WIDR/iNOS and melanoma cells in a dose-dependent fashion. The IC50, calculated from WIDR/iNOS cells (for which the only significant source of measurable NO is exogenously-supplied iNOS, was 595 μM (Fig 2B). The decrease in NO production by L-nil was not due to cytotoxicity, as viability of melanoma cells was not significantly affected by L-nil after up to 72 hours incubation (Fig 2D).

To test whether L-nil could reach a biologically relevant and therapeutic concentration *in vivo*, C57BL/6 mice received L-nil (0.15%) in drinking water before intraperitoneal challenge with LPS, a strong inducer of iNOS-dependent NO production from resident macrophages. L-nil treatment resulted in a strong decrease in serum nitrite levels after LPS challenge (Fig 2C), demonstrating the ability of orally administered L-nil to inhibit iNOS activity *in vivo*.

Targeted inhibition of iNOS antagonizes human melanoma growth *in vivo* and extends survival of tumor-bearing mice

We provided L-nil (0.15% in drinking water) or plain drinking water control to NOD/SCID mice bearing mel624 xenografts beginning on day 3 after tumor implantation. L-nil suppressed tumor growth for as long as the inhibitor was supplied in drinking water (4 weeks; Fig 3A). While the tumor resumed growth after discontinuation of treatment, L-nil treated mice survived significantly longer than untreated mice (Fig 3B). Another iNOS antagonist, 1,3-PBIT had a similar effect on mel624 growth when administered in drinking water (Fig 3C), suggesting that the anti-tumor effect of L-nil is due to iNOS inhibition rather than non-specific cytotoxicity or activity against non-NOS targets. Neither L-nil nor 1,3-PBIT caused any outward signs of toxicity in mice (behavioral changes, reduction in food or water intake, ruffled fur, hunched posture) after 4 weeks at the indicated concentration. There was no significant difference in body weight among control, L-nil, and 1,3-PBIT groups (Fig 3D) at the indicated doses; however wasting and behavioral changes were seen at higher doses of 1,3-PBIT.

iNOS inhibition results in decreased intratumoral microvessel density, downregulation of Bcl-2, and increased intratumoral apoptosis *in vivo*

As expected, treatment with L-nil did not appreciably alter *in vivo* expression of iNOS protein levels in melanoma xenografts, but reduced staining for nitrotyrosine confirmed the inhibition of intratumoral NO levels (Fig 4). Because NO is known to have angiogenic activity via induction of VEGF expression, we examined microvessel density in mel624 xenografts by immunohistochemistry for the vascular endothelial marker CD31 (Fig 4). After 19 days of L-nil treatment there was a significant (p=0.006) decrease in density of CD31+ microvessels in L-nil-treated mice, although the vessels' diameter was significantly greater (insert; average of 27 +/−2 pixels versus 10 +/−1 pixels in diameter). Because NO

has been suggested to inhibit apoptosis in human melanoma cells *in vitro*(21), we next examined the density of apoptotic (TUNEL+) cells in xenografts from L-nil-and control-treated mice (Fig 5A). Tumors from L-nil-treated mice contained approximately 3-fold more TUNEL+ cells than tumors from control mice, suggesting that the decreased growth of xenografts is at least in part due to a higher rate of cell death. Staining of serial sections with TUNEL and the vascular marker CD31 did not reveal consistent co-localization of TUNEL staining and CD31 (Fig 5A), as would be expected if endothelial cells were undergoing frequent apoptosis. Distribution of apoptotic cells was also not restricted to areas lacking vessel growth.

To further explore the possible mechanisms of tumor inhibition by L-nil, we measured the protein and phospho-protein expression of 59 proteins involved in signal transduction and cell survival pathways by reverse phase protein arrays (RPPA) [Table S1]. Two tumors were analyzed for each treatment, and multiple samples from each tumor were analyzed to control for intratumoral heterogeneity. This analysis demonstrated consistent decreases in multiple proteins, including several components of the PI3K-AKT signaling pathway, although we did not observe changes in phosphorylated AKT itself (Supplemental Figure 1). A potential link between iNOS inhibition and increased apoptosis in tumors from L-nil treated mice was suggested by a marked decrease in Bcl-2 expression levels which was confirmed by Western blotting analysis (Fig 5B). Bcl-2 is not only a critical regulator of cell death in response to a variety of stimuli, but its post-translational stability is also known to be regulated by NO via nitrosylation of key cysteine residues(14). This mechanism is supported by the observation that prolonged treatment of A375 melanoma cells with 1mM L-nil almost completely abolished Bcl-2 expression (Fig 5C).

Combination therapy with cisplatin + L-nil is effective against human melanoma cell lines *in vivo*

NO is known to affect signal transduction pathways regulating apoptosis (Bcl-2, caspase III, p53, and other survival and death pathways), and depletion of NO with the chemical NO scavenger PTIO has been shown to enhance sensitivity of human melanoma cells to cisplatin *in vitro*(21). Since we found that L-nil downregulated Bcl-2 expression in melanoma cells *in vivo*, we hypothesized that L-nil treatment would potentiate cytotoxic therapy of melanoma. Since resistance to conventional cytotoxic agents is a common clinical problem, we used both a relatively cisplatin-sensitive human melanoma line (A375), and the line mel624 which is 3–4-fold more resistant to cisplatin (Fig 6A). While neither cell line was sensitive to L-nil treatment alone (Fig 2C) *in vitro*, pretreatment of A375 cells with L-nil for 5 days increased sensitivity of cells to cisplatin-induced killing (Fig 6B).

We then tested combination therapy with L-nil plus cisplatin against human melanoma *in vivo*. While cisplatin or L-nil alone only partially suppressed the growth of established mel624 and A375, combination therapy with L-nil and cisplatin inhibited growth of mel624 and A375 more efficiently than either drug alone (Fig 6C) without additional toxicity. Although mice received only a single three-dose course of cisplatin treatment, continued treatment with L-nil alone was sufficient to suppress tumor growth.

DISCUSSION

While inflammation plays a well-established role in the initiation and progression of certain cancers, the ability of proinflammatory molecules to support the persistence of established cancer is a relatively recent observation. The present data confirm the hypothesis that iNOS is one such inflammatory mediator, capable of promoting the survival and proliferation of human melanoma cells *in vivo*. More importantly, we demonstrate that iNOS can be readily

targeted in melanoma without overt toxicity, and that iNOS inhibition reverses the chemoresistance of human melanoma.

Our data are consistent with previous studies, mostly *in vitro*, which demonstrate an effect of NOS inhibition on tumor growth, survival, or both(30–33). Our study is among the first to demonstrate dramatic anti-tumor activity of iNOS-selective inhibitors *in vivo*, and feasibility of combination treatment of cancer combining targeted iNOS inhibition and cytotoxic chemotherapy. There are several potential mechanisms by which iNOS antagonists may inhibit tumor growth, either directly or by sensitizing cells to other forms of stress, such as hypoxia or ROS-mediated stress. Mechanisms by which iNOS inhibition may affect the resistance of cancer cells to apoptosis include interference with PI3K/AKT-mediated overexpression of survivin (34,35); or reversal of caspase inactivation(15)or Bcl-2 stabilization mediated by s-nitrosylation of these proteins(14). Indeed, we observed that L-nil induced downregulation of Bcl-2 protein expression *in vivo* and *in vitro*, suggesting that this is one mechanism by which iNOS inhibition may enhance susceptibility of cancer cells to apoptosis. L-nil's relative lack of direct cytotoxicity *in vitro* (Fig 2C) despite causing markedly increased tumor apoptosis *in vivo* may reflect the relative absence of stressful stimuli (hypoxia, acidosis, cytokines, etc.) *in vitro* which might force melanoma cells to depend on Bcl-2 expression for survival.

NO has well-established pro-angiogenic properties, and stimulation of angiogenesis is one proposed mechanism by which iNOS expression may support tumor growth (36), (37). We observed a nearly two-fold decrease in tumor microvessel density in tumors from L-nil-treated mice, although the average caliber of the remaining vessels was greater (see inset, Fig 4, lower panels). As both suppression of vascularization and increased apoptosis may lead to a diminished overall rate of tumor growth, they may act additively or synergistically to cause the observed significant decrease in tumor growth *in vivo*.

Another potential mechanism of tumor growth suppression is interference with the NO-dependent proliferation of tumor cells. While relatively few studies have attempted to disentangle the dual effect of NO on tumor cell survival and proliferation, NO has been shown to increase proliferation of human breast cancer cells *in vitro* via stimulation of the AKT/mTOR pathway and downstream upregulation of cyclin D1(38). It is interesting that of the nearly 60 proteins and phospho-proteins we examined by RPPA, multiple proteins in the mTOR pathway, including P70S6K, and mTOR were significantly and coordinately down-regulated by L-nil treatment *in vivo* (Supplemental Figure 1). We are currently investigating the effect of iNOS/NO inhibition on melanoma proliferation and regulation of the AKT/mTOR and other proliferation/survival pathways.

When we tested the *in vivo* anti-tumor efficacy of iNOS inhibition, alone and in combination with cisplatin, both lines tested exhibited nearly complete sensitivity to combination treatment with doses of L-nil and cisplatin that were only partly therapeutic as single agents. Since melanoma quickly acquires resistance to conventional chemotherapy in the clinical setting, restoring the efficacy of cytotoxic chemotherapy by adding a well-tolerated targeted agent to the regimen is an exciting possibility that deserves testing in clinical trials. It is notable that although cisplatin was administered for only a single three-dose course, the beneficial effect of combination therapy persisted for significantly longer, so long as L-nil was continued. This suggests the potential for therapeutic regimens which utilize up-front or periodic combination chemo/targeted therapy followed by maintenance therapy with a relatively non-toxic targeted iNOS inhibitor.

The use of L-nil and related compounds *in vivo* seems promising because of the magnitude of tumor inhibition (by a factor of 3–5-fold at 4 weeks) and its favorable toxicity profile.

While important to note that we did not monitor changes in blood pressure, a potential side effect of chronic treatment with NO-active compounds, we did not observe any overt L-nil toxicity at doses up to 0.2 % (7.7 mM in drinking water) when administered for up to 4 weeks. This is despite our observation that L-nil is a relatively weak inhibitor *in vitro*, with an IC50 of nearly 600 μM (Fig 2A and 2B). This is significantly higher than the published IC50 values for L-nil in cell-free enzyme assays(22), and likely reflect the need for active transport of the molecule across the cell membrane(39)as well as degradation in aqueous solution over the course of 24 hours culture (Cayman Chemical product information). Variations in the efficiency of transport may also contribute to differences in the efficacy of L-nil-mediated NO suppression among our panel of cell lines. In our *in vitro* experiments, the predicted concentration of L-nil required to suppress > 90% NO production varied from 1 to >3mM. This is quite similar to the theoretical concentration of L-nil in tissues *in vivo* during treatment (assuming complete absorption of the drug in a drinking water volume of 6 mL/day) which would be 2.13mM. Since complete drug distribution into the bloodstream after oral administration is unlikely, the tumor suppressive effects observed *in vivo* are likely due to partial, rather than complete, inhibition of iNOS; this is also supported by the partial inhibition of intratumoral nitrotyrosine deposition (Fig 4) and LPS-induced nitrite production *in vivo* (Fig 2D) after treatment with 0.1% L-nil. This suggests that it may be possible to more efficiently inhibit iNOS by escalating the dose of L-nil, potentially improving its anti-tumor efficacy. As L-nil and similar NOS inhibitors have previously been the subject of non-cancer human clinical trials(40–42), these findings have strong translational potential.

Our results do not exclude the possibility that the anti-tumor activity of L-nil is enhanced by inhibition of iNOS in other (host) cell types *in vivo*. This is particularly relevant since there is little direct cytotoxic effect of L-nil *in vitro*. iNOS can be expressed by host stromal, endothelial, and bone marrow-derived cells present in tumors *in vivo*, and inhibition of NO production by any of these cell types could indirectly affect tumor growth and viability. We are currently working to determine what role, if any, host-derived iNOS plays a role in the antitumor effect of L-nil on melanoma xenografts *in vivo*. Another limitation of our experimental system is reliance on small-molecule iNOS-selective inhibitors to implicate iNOS-derived NO in the growth and resistance to cytotoxicity of tumor cells. No chemical inhibitor is completely selective, and in fact many so-called “targeted” agents can act on a relatively broad set of molecular targets (43). However, the similar anti-tumor activity of two structurally dissimilar iNOS inhibitors, L-nil and 1,3 PBIT, (Fig 3C) suggests that iNOS is indeed the primary target of these treatments. Finally, although NO has been shown to suppress T cell-dependent immune responses, our immunodeficient human/mouse xenograft model is not ideal for studying effects of iNOS inhibition on tumor-mediated immunosuppression and interference with endogenous anti-tumor immunity.

In summary, this study clearly demonstrates the robust anti-tumor effect of iNOS-selective small-molecule inhibitors in a preclinical human melanoma model, and their ability to synergize with conventional cytotoxic chemotherapy *in vivo*. The lack of appreciable toxicity associated with chronic L-nil treatment, and its ability to enhance the efficacy of cisplatin, suggest that iNOS inhibition, alone or in combination with cytotoxic chemotherapy, deserves evaluation in clinical trials for melanoma and other solid tumors. More generally, the regulation of inflammatory mediators in cancer is a promising approach to targeted cancer therapy and reversal of chemoresistance.

Supplementary Material

Refer to Web version on PubMed Central for supplementary material.

Acknowledgments

The authors thank Dr. Nina Chinosornvatana, MD (Department of Otolaryngology, Mount Sinai School of Medicine) for assistance in performing experiments which contributed to figure 6B, as well as Ajish George (Department of Biomedical Sciences, School of Public Health, SUNY Albany) for helpful advice regarding molecular pathway analysis. For MRI analysis we are grateful to the MD Anderson Small Animal Imaging Facility, supported by a MD Anderson Center Support Grant (CA016672). We also acknowledge the following grant support: P50 CA09349(PP-DRP5 and PP-CDP5), U.T. MD Anderson Cancer Center SPORE in Melanoma(Grimm, Overwijk, Sikora); NIDCD National Research Service Award Institutional Training Grant T32 D007367 (Gelbard, Sikora); American Head and Neck Society/American Academy of Otolaryngology Young Investigator Award (Sikora); NCI#CA16672 supporting the MDACC Characterized Cell Line Core and RPPA Core laboratories.

References

1. Kundu JK, Surh Y. Inflammation: gearing the journey to cancer. Mutat Res 2008;659:15–30. [PubMed: 18485806]
2. Li L, Xu H. Inducible nitric oxide synthase, nitrotyrosine and apoptosis in gastric adenocarcinomas and their correlation with a poor survival. World J Gastroenterol 2005;11:2539–2544. [PubMed: 15849807]
3. Vakkala M, et al. Inducible nitric oxide synthase expression, apoptosis, and angiogenesis in in situ and invasive breast carcinomas. Clin Cancer Res 2000;6:2408–2416. [PubMed: 10873093]
4. Cianchi, F., et al. Inducible Nitric Oxide Synthase Expression in Human Colorectal Cancer Correlation with Tumor Angiogenesis. ASIP; 2003.
5. Brennan PA, et al. Inducible nitric oxide synthase: Correlation with extracapsular spread and enhancement of tumor cell invasion in head and neck squamous cell carcinoma. Head Neck 2008;30:208–14. [PubMed: 17657783]
6. Pukkila MJ, et al. Inducible nitric oxide synthase expression in pharyngeal squamous cell carcinoma: relation to p53 expression, clinicopathological data, and survival. Laryngoscope 2002;112:1084–8. [PubMed: 12160278]
7. Albina JE, Reichner JS. Role of nitric oxide in mediation of macrophage cytotoxicity and apoptosis. Cancer Metastasis Rev 1998;17:39–53. [PubMed: 9544422]
8. Thomas DD, et al. Heme proteins and nitric oxide (NO): the neglected, eloquent chemistry in NO redox signaling and regulation. Antioxid Redox Signal 2003;5:307–317. [PubMed: 12880485]
9. Landar A, Darley-Usmar VM. Nitric oxide and cell signaling: modulation of redox tone and protein modification. Amino Acids 2003;25:313–321. [PubMed: 14661093]
10. Gow AJ, Farkouh CR, Munson DA, Posencheg MA, Ischiropoulos H. Biological significance of nitric oxide-mediated protein modifications. Am J Physiol Lung Cell Mol Physiol 2004;287:L262–268. [PubMed: 15246980]
11. Dai Fukumura SK, Jain RK. The role of nitric oxide in tumour progression. NATURE REVIEWS/ CANCER 2006;6:521.
12. Ekmekcioglu S, Tang C, Grimm EA. NO news is not necessarily good news in cancer. Curr Cancer Drug Targets 2005;5:103–15. [PubMed: 15810875]
13. Wink DA, Ridnour LA, Hussain SP, Harris CC. The reemergence of nitric oxide and cancer. Nitric Oxide 2008;19:65–67. [PubMed: 18638716]
14. Azad N, et al. S-Nitrosylation of Bcl-2 Inhibits Its Ubiquitin-Proteasomal Degradation: A NOVEL ANTIAPOPTOTIC MECHANISM THAT SUPPRESSES APOPTOSIS. Journal of Biological Chemistry 2006;281:34124. [PubMed: 16980304]
15. Mannick, JB., et al. S-Nitrosylation of mitochondrial caspases. Rockefeller Univ Press; 2001.
16. Bogdan C. Nitric oxide and the immune response. NATURE IMMUNOLOGY 2001;2:907–916. [PubMed: 11577346]
17. American Cancer Society. Cancer Facts and Figures: 2009. 2009.
18. Massi D, et al. Inducible nitric oxide synthase expression in benign and malignant cutaneous melanocytic lesions. J Pathol 2001;194:194–200. [PubMed: 11400148]
19. Ekmekcioglu S, et al. Tumor iNOS predicts poor survival for stage III melanoma patients. Int J Cancer 2006;119:861–6. [PubMed: 16557582]

20. Ekmekcioglu S, et al. Inducible nitric oxide synthase and nitrotyrosine in human metastatic melanoma tumors correlate with poor survival. Clin Cancer Res 2000;6:4768–75. [PubMed: 11156233]
21. Tang C, Grimm EA. Depletion of endogenous nitric oxide enhances cisplatin-induced apoptosis in a p53-dependent manner in melanoma cell lines. J Biol Chem 2004;279:288–98. [PubMed: 14576150]
22. Moore WM, et al. L-N6-(1-iminoethyl)lysine: a selective inhibitor of inducible nitric oxide synthase. J Med Chem 1994;37:3886–3888. [PubMed: 7525961]
23. Xie K, et al. Transfection with the inducible nitric oxide synthase gene suppresses tumorigenicity and abrogates metastasis by K-1735 murine melanoma cells. J Exp Med 1995;181:1333–1343. [PubMed: 7535333]
24. Berkels R, Purol-Schnabel S, Roesen R. A new method to measure nitrate/nitrite with a NO-sensitive electrode. J Appl Physiol 2001;90:317–320. [PubMed: 11133924]
25. Bryan NS, Grisham MB. Methods to detect nitric oxide and its metabolites in biological samples. Free Radic Biol Med 2007;43:645–657. [PubMed: 17664129]
26. Seki H, et al. Differential protective action of cytokines on radiation-induced apoptosis of peripheral lymphocyte subpopulations. Cell Immunol 1995;163:30–36. [PubMed: 7758128]
27. Tibes R, et al. Reverse phase protein array: validation of a novel proteomic technology and utility for analysis of primary leukemia specimens and hematopoietic stem cells. Mol Cancer Ther 2006;5:2512–2521. [PubMed: 17041095]
28. Koziol JA, Maxwell DA, Fukushima M, Colmerauer ME, Pilch YH. A distribution-free test for tumor-growth curve analyses with application to an animal tumor immunotherapy experiment. Biometrics 1981;37:383–90. [PubMed: 7272422]
29. Jenkins DC, et al. Human colon cancer cell lines show a diverse pattern of nitric oxide synthase gene expression and nitric oxide generation. Br J Cancer 1994;70:847–849. [PubMed: 7524602]
30. Wang G, Ji B, Wang X, Gu J. Anti-cancer effect of iNOS inhibitor and its correlation with angiogenesis in gastric cancer. World J Gastroenterol 2005;11:3830–3833. [PubMed: 15991277]
31. Shang Z, Li Z, Li J. In vitro effects of nitric oxide synthase inhibitor L-NAME on oral squamous cell carcinoma: a preliminary study. Int J Oral Maxillofac Surg 2006;35:539–543. [PubMed: 16497478]
32. Madhunapantula SRV, et al. PBISe, a novel selenium-containing drug for the treatment of malignant melanoma. Molecular Cancer Therapeutics 2008;7:1297. [PubMed: 18483317]
33. Malone JM, Saed GM, Diamond MP, Sokol RJ, Munkarah AR. The effects of the inhibition of inducible nitric oxide synthase on angiogenesis of epithelial ovarian cancer. American Journal of Obstetrics & Gynecology 2006;194:1110. [PubMed: 16580304]
34. Engels K, et al. NO signaling confers cytoprotectivity through the survivin network in ovarian carcinomas. Cancer Res 2008;68:5159–5166. [PubMed: 18593915]
35. Fetz V, et al. Inducible NO synthase confers chemoresistance in head and neck cancer by modulating survivin. Int J Cancer 2009;124:2033–2041. [PubMed: 19130609]
36. Roy HK, et al. Inducible nitric oxide synthase (iNOS) mediates the early increase of blood supply (EIBS) in colon carcinogenesis. FEBS Letters 2007;581:3857–3862. [PubMed: 17658518]
37. Singh RP, Agarwal R. Inducible nitric oxide synthase-vascular endothelial growth factor axis: a potential target to inhibit tumor angiogenesis by dietary agents. Curr Cancer Drug Targets 2007;7:475–483. [PubMed: 17691907]
38. Pervin S, Singh R, Hernandez E, Wu G, Chaudhuri G. Nitric oxide in physiologic concentrations targets the translational machinery to increase the proliferation of human breast cancer cells: involvement of mammalian target of rapamycin/eIF4E pathway. Cancer Res 2007;67:289–299. [PubMed: 17210710]
39. Hatanaka T, et al. Na+ -and Cl−-coupled active transport of nitric oxide synthase inhibitors via amino acid transport system B(0,+). J Clin Invest 2001;107:1035–1043. [PubMed: 11306607]
40. Hansel TT, et al. A selective inhibitor of inducible nitric oxide synthase inhibits exhaled breath nitric oxide in healthy volunteers and asthmatics. FASEB J 2003;17:1298–1300. [PubMed: 12738811]

41. Lassen LH, Christiansen I, Iversen HK, Jansen-Olesen I, Olesen J. The effect of nitric oxide synthase inhibition on histamine induced headache and arterial dilatation in migraineurs. Cephalalgia 2003;23:877–886. [PubMed: 14616929]

42. Freedman BI, et al. Design and baseline characteristics for the aminoguanidine Clinical Trial in Overt Type 2 Diabetic Nephropathy (ACTION II). Control Clin Trials 1999;20:493–510. [PubMed: 10503809]

43. Karaman MW, et al. A quantitative analysis of kinase inhibitor selectivity. Nat Biotechnol 2008;26:127–132. [PubMed: 18183025]

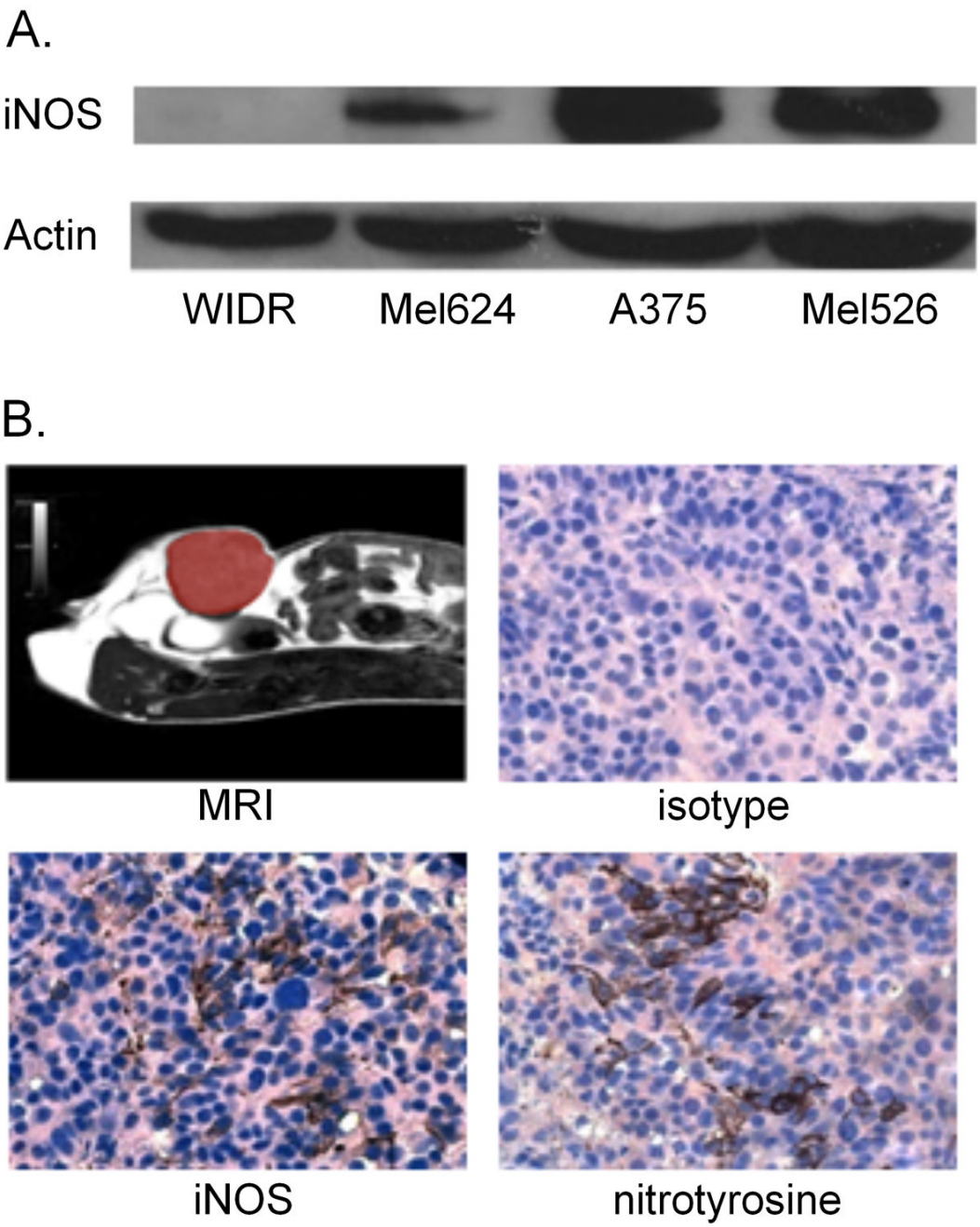

Figure 1. Human melanoma lines constitutively express iNOS and make NO in vitro and in vivo

A. Human melanoma lines mel624, A375, and mel526, and the iNOS-negative colon cancer line WiDR were assessed by Western blot for iNOS protein expression. **B.** 5×10^6 A375 melanoma cells were injected subcutaneously into recipient NOD/SCID mice and allowed to form 0.5 cm tumors. Xenografts were then harvested and sections stained by immunohistochemistry for iNOS and the stable NO reaction product nitrotyrosine. Representative MRI (tumor in false color) and immunohistochemistry results are shown.

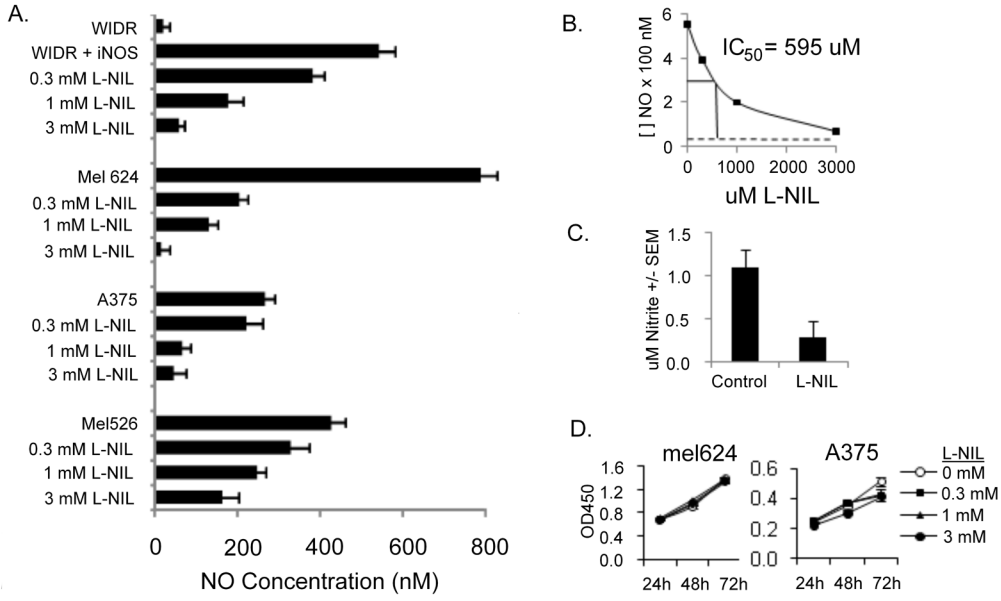

Figure 2. The iNOS-selective competitive antagonist L-nil blocks iNOS-derived NO production in vitro and in vivo without affecting cell viability

A. Human melanoma lines mel624, A375, mel526; or colon cancer line WIDR or WIDR transfected with iNOS plasmid were incubated for 72 hours with the indicated concentrations of L-nil, and NO released into the supernatant measured using the nitrite reconversion method. **B.** The effect of L-nil on NO production by WIDR+iNOS plasmid was used to determine the IC_{50} of L-nil in the cell culture system. **C.** Serum was collected 7 hours after intraperitoneal LPS injection of C57BL/6 mice (4 per group) pre-treated for 48 hours with 0.1% L-nil in drinking water (L-nil) or plain drinking water (control) Nitrite levels were determined using the Griess assay. **D.** Mel624 or A375 melanoma cells were cultured for the indicated length of time in medium containing varying concentrations of L-nil and proliferation was measured by XTT assay.

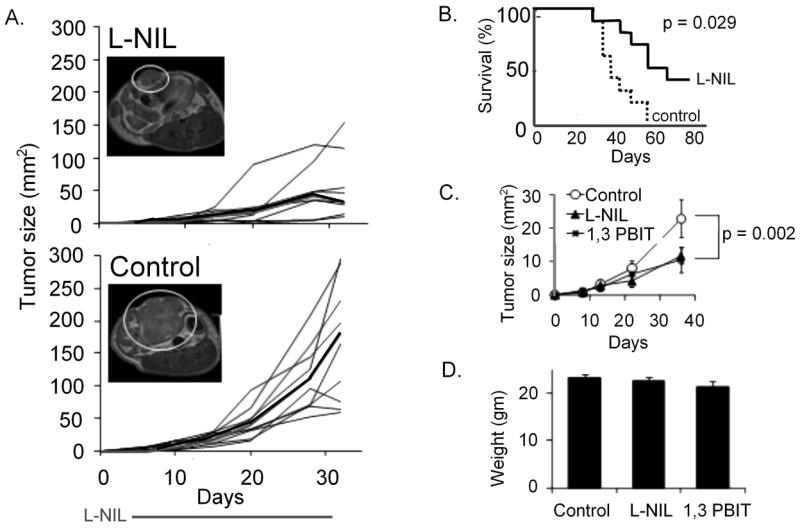

Figure 3. Orally-administered selective iNOS antagonists suppress the growth of human melanoma and extend survival without overt toxicity in an immunodeficient mouse xenograft model

A. 5×10^6 mel624 cells were injected subcutaneously on day 0. Starting on day 3, mice were treated with 0.15% L-nil in drinking water, or plain water control, for 28 days. Tumor sizes are expressed as mm^2; each black line represents an individual mouse, median size is with a bold line. Right panels show representative MRI pictures of day 22 tumors from L-nil-(top) and control-(bottom) treated mice. Data is representative of three experiments. **B.** Kaplan-Meier survival estimates for control-and 0.15% L-nil-treated mel624-bearing mice. **C.** Using the experimental design described in 3A, mel624-bearing mice were treated with 0.15% L-nil or 0.2% 1,3-PBIT in drinking water or plain drinking water control for 28 days starting on day 3. Tumor sizes are expressed as mean +/− SEM. Data is representative of two experiments. **D.** Mice were weighed after 21 days treatment with 0.15% L-nil or 0.2% PBIT in drinking water, or plain water control.

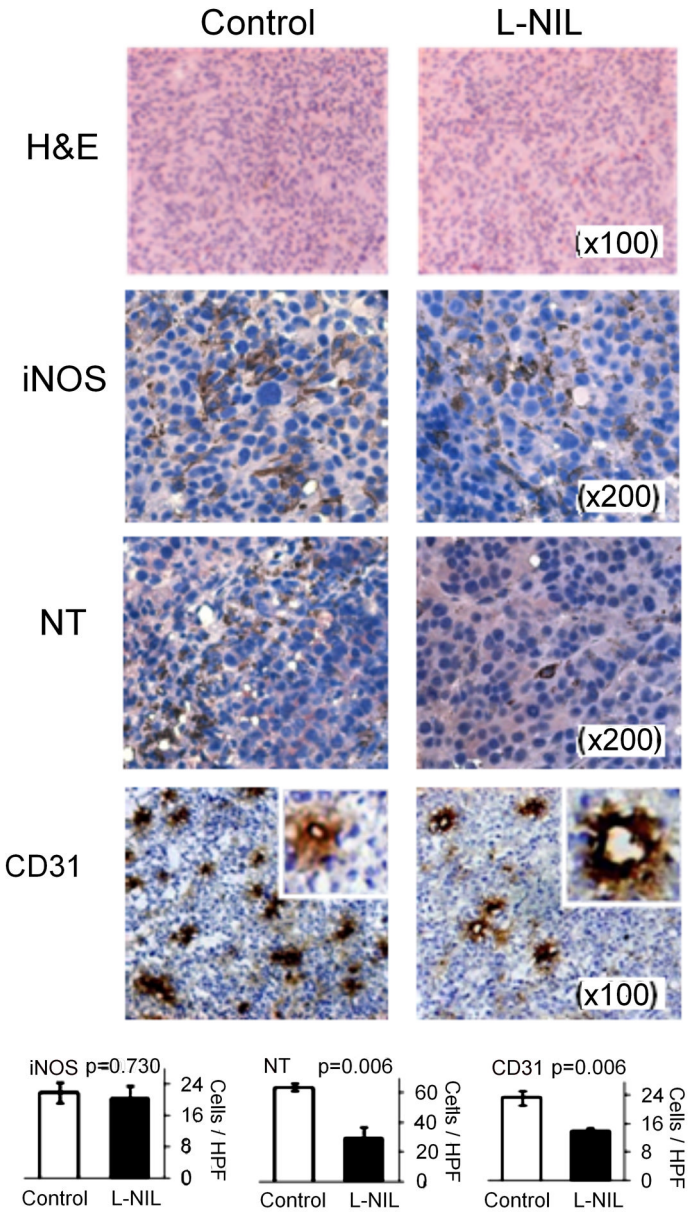

Figure 4. Oral L-nil treatment inhibits intratumoral nitrotyrosine formation, and decreases tumor microvessel density

Mel624-bearing mice were treated for 14 days with 0.15% L-nil in drinking water or plain water control prior to sacrifice, harvest of xenografts, and hematoxalin and eosin staining (top), or immunohistochemical staining for iNOS, nitrotyrosine (NT), or the vascular marker CD31. Representative images are shown at the indicated original magnifications, except the insert pictures of representative CD31-stained vessels at 400X. Computer-assisted quantitation of images is shown to the right.

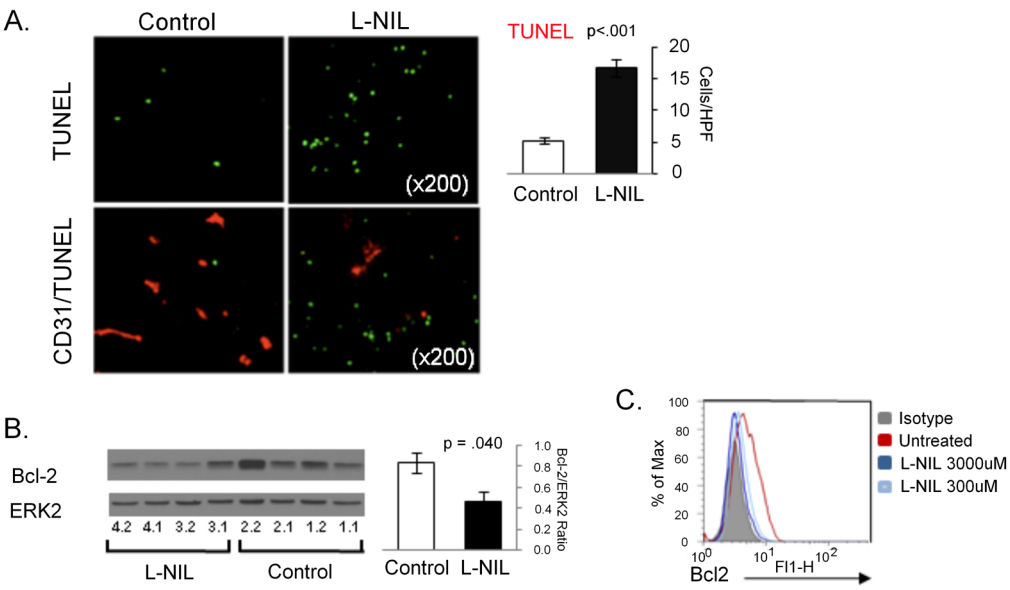

Figure 5. L-nil downregulates Bcl-2 expression and induces intratumoral apoptosis in vivo

A. Mel624 xenografts were harvested from mice after treatment with 0.15% L-nil or plain water control for 14 days. Paraffin-embedded slides were subjected to TUNEL analysis of apoptotic cells (top), or double-staining for TUNEL and the vascular marker CD31(bottom). Representative images are shown on the left and quantitation of TUNEL staining on the right. **B.** Western blot analysis mel624 xenograft lysates was performed to confirm downregulation of Bcl-2 expression in tumors from L-nil treated mice (2 replicates of 2 tumors per group). The bar graph shows quantitation of Bcl-2 levels (normalized to Erk2 protein expression) in tumors from control and L-nil treated mice. **C.** 5×10^4 A375 cells were cultured in 48 well plates for 3 days with the indicated concentration of L-nil, at which time the medium and inhibitor were replenished and cells cultured for an additional 2 days prior to immunostaining for intracellular Bcl-2 and analysis by flow cytometry.

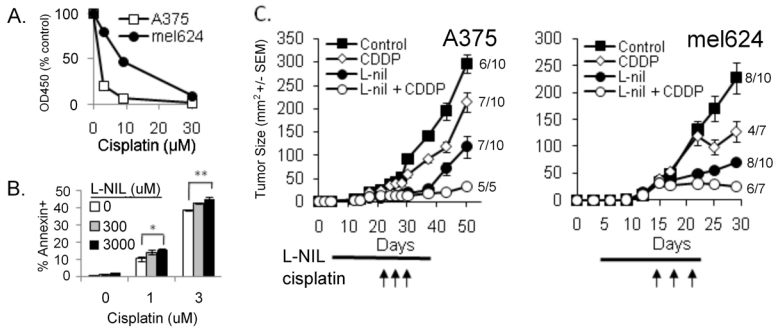

Figure 6. L-nil enhances sensitivity of human melanoma cells to anti-tumor effect of cisplatin in vitro and in vivo

A. A375 and mel624 cells were treated with the indicated concentrations of cisplatin for 48 hours and proliferation was measured by XTT assay. Data are presented as mean +/− SEM and are representative of three independent experiments. **B.** 2×10^4 A375 melanoma cells were cultured in the indicated concentration of L-nil for 3 days. On day 3, the medium was discarded and cells were incubated for another 48 hours in fresh media with the indicated concentration of L-nil and/or cisplatin. Cells were then trypsinized and cell death was assessed by annexin V staining and flow cytometry. Data are presented as mean +/− SEM and are representative of 3 independent experiments. *p=0.012, **p=0.003) **C.** SCID-NOD mice were injected subcutaneously with 5×10^6 A375 or mel624 cells, and treated with 0.2% L-nil for the indicated time, starting on day 3. Cisplatin was given as three intraperitoneal injections of 2.5 mg/kg (A375) or 6 mg/kg (mel624) spaced three days apart, beginning on day 13 (mel624) or day 25 (A375). The numbers to the right of each curve give the fraction of surviving mice. For A375 p<0.001 for CDDP+L-nil vs. CDDP alone; p=0.009 for CDDP +L-nil vs. L-nil alone. For mel624 p<0.001 for CDDP+L-nil vs. CDDP alone; p=0.010 for CDDP+L-nil vs. L-nil alone on day 30.